Equivalent Circuit Model for Multi-Electrode Semiconductor Optical Amplifiers and Analysis of Inline Photodetection in Bidirectional Transmissions

A. Sharaiha and M. Guegan

***Abstract*—A rate equation model for static and dynamic behavior for bidirectional transmission in a multisection semiconductor optical amplifier (SOA) is presented. The rate equations for each section have been implemented on an electrical simulator. Here, we have used the model to study the inline photodetection in presence of bidirectional transmission. Small signal photodetection response in presence of co- and contrapropagating signals is given. The photodetection crosstalk expression in bidirectional transmission has also been reported. Simultaneous bidirectional photodetection experiments using a three-electrode SOA show good agreement between measured crosstalk and simulated results obtained by harmonic balance method. A photodetection response nearly free of crosstalk has been obtained for certain operating conditions due to the cross gain modulation between contrapropagating signals.**

***Index Terms*—Bidirectional detection, equivalent circuit, optical duplex transmission, photodetectors, semiconductor optical amplifier (SOA), SOA device modeling.**

I. Introduction

SEMICONDUCTOR optical amplifiers (SOA's) are likely to play an important role in future optical communication links. They have demonstrated their multifunctional capability by combining optical amplification with either modulation, photodetection, gating, and wavelength conversion [1]–[9]. Using multi-electrode SOA permit to optimize and to increase SOA applications [10]–[14]. In optical duplex transmission, a simultaneous inline photodetection has been reported [14] by using a two-electrode SOA. The signal detection can be performed over all the SOA spectral −3 dB bandwidth, which can be interesting in WDM applications.

In this paper, we present a model for multi-electrode SOA's in presence of co- and contrapropagating signals. This numerical model for a multi-electrode SOA is based on that used previously [15]–[20]. In our work, the SOA is divided into M sections and we consider that all fields may be approximated by the propagation of plane waves and the carrier density is regarded as a constant in each SOA section. A rate equation model is used to describe the dynamics of the carrier concentrations in each section. In each one, analytical expressions of the average photon densities for amplified spontaneous emission, and for co– and contradirectional optical input signals are given. The rate equations of the SOA model are then transformed under the form of an equivalent circuit [21]–[23], which allows the use of a commercial electrical simulator.

Here we have applied the model to study the inline photodetection in presence of bidirectional transmission but it can also be used to simulate other SOA functions as modulation, switching and wavelength conversion. Small signal photodetection response in presence of co and contrapropagating signals is given. The photodetection crosstalk expression in bidirectional transmission has also been reported. Experimental measurements of photodetection crosstalk are obtained by using a three-electrode SOA and are compared with simulation.

Manuscript received June 1, 1999; revised January 21, 2000. This work was supported by the Brittany Region in France.

The authors are with the Ecole Nationale d'Ingénieurs de Brest, Laboratoire RESO, Technopôle Brest, Iroise, BP 30815, 29608 BREST cedex, France (e-mail: sharaiha@enib.fr; mguegan@enib.fr).

Publisher Item Identifier S 0733-8724(00)03746-4.

II. Equivalent Circuit Model for a Multi-Electrode SOA

A. Cavity Model

A multi-electrode SOA with N contacts can be divided into M sections excluding the two amplifier facets (Fig. 1). The input facet, of field reflectance r_1, and transmittance t_1 is situated at $z = 0$. It receives at $z = 0$ an input field $F^{+}_{in,\,i}$ at the wavelength λ_i. The corresponding reflected field is noted $F^{-}_{r,\,i}$. The output facet, of field reflectance r_2, and transmittance t_2 is situated at $z = L$ and emits a field $F^{+}_{\mathrm{out},\,i}$. The fields amplitude of the amplified signal due to the optical gain in the active region of the kth section $F_{k,\,i}$ and the intensity of the amplified spontaneous emission (ASE) coupled to the mth optical mode $I_{\mathrm{spon},\,k,\,m}$ can be given in the z-direction by [15], [17], [20]

$$F^{\pm}_{k,\,i}(z) = A^{\pm}_{k} \exp\left(\pm g_{n,\,k,\,i}\left(z - z^{\mp}_{k}\right)/2\right) \exp\left(\mp i k_{k,\,i}\left(z - z^{\mp}_{k}\right)\right) \tag{1}$$

$$I^{\pm}_{\mathrm{spon},\,k,\,m}(z) = \frac{\beta_m R_{\mathrm{spon},\,k} E_m}{2 g_{n,\,k,\,m}} \left(C^{\pm}_{k,\,m} \exp\left(\pm g_{n,\,k,\,m}\left(z - z^{\mp}_{k}\right)\right) - 1\right) \tag{2}$$

where

superscript + or −	corresponding to whether they are moving in the positive or negative z-directions;
β_m	spontaneous emission coupling factor;
$R_{\mathrm{spon},\,k}$	spontaneous emission rate;

E_m	photon energy;
k_k	wavenumber;
$g_{n,k}$	net power gain given by $g_{n,k} = \Gamma g_{m,k} - \alpha$ where Γ is the confinement factor for the intensity of the fundamental wave guide mode;
α	internal loss;
$g_{m,k}$	material gain.

The material gain is assumed to shift linearly with the carrier density.

The state of the field at any given abscissa z is related to the state of the field at any other abscissa $z+\Delta z$ by transfer matrix [19], [24]

$$\begin{bmatrix} F^{+}_{k,i}(z) \\ F^{-}_{k,i}(z) \end{bmatrix} = \begin{bmatrix} G^{-1/2}_{si,k}\exp(ik_k\Delta z) & 0 \\ 0 & G^{1/2}_{si,k}\exp(-ik_k\Delta z) \end{bmatrix} \cdot \begin{bmatrix} F^{+}_{k,i}(z+\Delta z) \\ F^{-}_{k,i}(z+\Delta z) \end{bmatrix} \tag{3}$$

where $G_{si,k} = \exp(g_{n,k,i}\Delta z)$ is the simple pass SOA gain at λ_i in the kth section for a Δz length.

The above relationship can be written in a more compact form as

$$\boldsymbol{F_k} = \boldsymbol{X_k}(\boldsymbol{\Delta z}).\boldsymbol{F_{k+\Delta z}} \tag{4}$$

where $\boldsymbol{F_k}$, $.\boldsymbol{F_{k+\Delta z}}$ represents the column matrix and $\boldsymbol{X_k}$ is the transfer matrix.

The relationship between F^{+}_{out} and F^{+}_{in} can be found through the iterative use of the transfer matrix relation in (4) and the transfer matrix of the SOA input and output facets [19]

$$\begin{bmatrix} F^{+}_{\text{in},i} \\ F^{-}_{r,i} \end{bmatrix} = \frac{1}{t_1 t_2}\begin{bmatrix} 1 & -r_1 \\ -r_1 & 1 \end{bmatrix}\prod_{j=1}^{M} X_j \begin{bmatrix} 1 & r_2 \\ r_2 & 1 \end{bmatrix}\begin{bmatrix} F^{+}_{\text{out},i} \\ 0 \end{bmatrix}. \tag{5}$$

From (5) the gain of the amplifier can be calculated as

$$G_i = \left|\frac{F^{+}_{\text{out},i}}{F^{+}_{\text{in},i}}\right|^2 = \frac{(1-R_1)(1-R_2)G_{si}}{(1-\sqrt{(R_1R_2)}G_{si})^2 + 4\sqrt{(R_1R_2)}G_{si}\sin^2\left(\sum_{k=1}^{M}\Phi_k\right)} \tag{6}$$

where $G_{si} = \prod_{j=1}^{M} G_{si,j}$ is the total simple pass SOA gain; $R_{1,2} = r^2_{1,2} = 1 - t^2_{1,2}$ and ϕ_k is the single-pass phase change in the kth section. In the limit of a single-section SOA, this result reduces to the well known expression for transmission of a Fabry–Perot cavity with gain [15], [17].

The average photon density for the signal at wavelength λ_i in the kth section $S^{+}_{k,i}$can be given by

$$S^{+}_{k,i} = \frac{1}{v_g E_i \Delta z_k}\int_{z^{-}_k}^{z^{+}_k}\left(\left|F^{+}_{k,i}(z) + F^{-}_{k,i}(z)\right|^2\right)dz \approx \frac{1}{v_g E_i \Delta z_k}\int_{z^{-}_k}^{z^{+}_k}\left(\left|F^{+}_{k,i}(z)\right|^2 + \left|F^{-}_{k,i}(z)\right|^2\right)dz \tag{7}$$

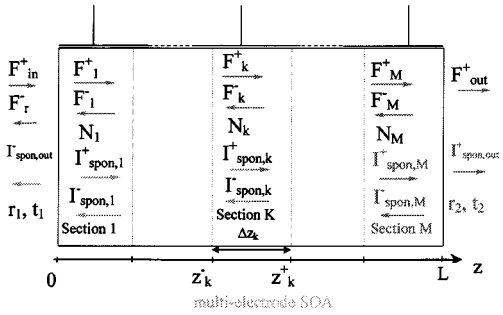

Fig. 1. Cavity model of a multi-electrode SOA divided into M sections. The signal field is denoted by $F^{\pm}$, the spontaneous intensity is given by $I^{\pm}$, and the carrier density by N_k.

where

E_i	is the photon energy at λ_i;
v_g	is the group velocity;
Δz_k	is the length of kth section.

We note in (7), that the interference terms between forward and backward traveling waves, $F^{\pm}_{k,i}$, have been neglected [15]–[17]. $F^{\pm}_{k,i}$ can then be expressed as a function of $F^{+}_{\text{out},i}$ through the iterative use of transfer matrix relation in (4)

$$\begin{bmatrix} F^{+}_{k,i}(z) \\ F^{-}_{k,i}(z) \end{bmatrix} = \frac{1}{t_2}X_k(z^{+}_k - z)\prod_{j=k+1}^{M} X_j\Delta z_j \begin{bmatrix} 1 & r_2 \\ r_2 & 1 \end{bmatrix}\begin{bmatrix} F^{+}_{\text{out},i} \\ 0 \end{bmatrix}. \tag{8}$$

By using (7) and (8), $S^{+}_{k,i}$ can be calculated and be written as

$$S^{+}_{k,i} = \frac{\Gamma G_i P_{in,i}}{v_g E_i (1-R_2) w d \Delta z_k g_{n,k,i}} \cdot \left(1 - G^{-1}_{si,k}\right)\left(\prod_{j=k+1}^{M} G^{-1}_{si,j} + R_2\prod_{j=k}^{M} G_{si,j}\right) \tag{9}$$

where $\prod_{j=k+1}^{M} G^{-1}_{si,j} = 1$ for $k = M$. w and d are, respectively, the width and thickness of the active region. The input power $P_{\text{in},i}$ is obtained from $P_{\text{in},i} = \Gamma^{-1}|F^{+}_{in,i}|^2 wd$. Equation (9) reduces to the corresponding result for single-section and two-section SOA [15]–[17].

In the case where an input field $F^{-}_{\text{in},i}$ arrives at $z = L$, the reflected field is $F^{+}_{r,i}$ and emits a field $F^{-}_{\text{out},i}$ at $z = 0$. The transfer matrix of the SOA becomes

$$\begin{bmatrix} 0 \\ F^{-}_{\text{out},i} \end{bmatrix} = \frac{1}{t_1 t_2}\begin{bmatrix} 1 & -r_1 \\ -r_1 & 1 \end{bmatrix}\prod_{j=1}^{M} X_j \begin{bmatrix} 1 & r_2 \\ r_2 & 1 \end{bmatrix}\begin{bmatrix} F^{+}_{r,i} \\ F^{-}_{in,i} \end{bmatrix}. \tag{10}$$

By similar development as in (7) and (8), we can obtain the average photon density in the kth section by

$$S^{-}_{k,i} = \frac{\Gamma G_i P_{in,i}}{v_g E_i (1-R_1) w d \Delta z_k g_{n,k,i}} \cdot \left(1 - G^{-1}_{si,k}\right)\left(\prod_{j=1}^{k-1} G^{-1}_{si,j} + R_1\prod_{j=1}^{k} G_{si,j}\right) \tag{11}$$

where $\prod_{j=1}^{k-1} G^{-1}_{si,j} = 1$ for $k = 1$.

In the case of multichannel amplification using SOA and in presence of co- and contrapropagating signals, the average photon density $\sum_\sigma S^{\pm}_{k,\sigma}$ in the kth section can be given by

$$\sum_\sigma S^{\pm}_{k,\sigma} = \frac{1}{v_g \Delta z_k} \int_{z_k^-}^{z_k^+} \cdot \left(\left| \sum_\sigma \frac{1}{\sqrt{E_\sigma}} F^+_{k,\sigma}(z) + \sum_\sigma \frac{1}{\sqrt{E_\sigma}} F^-_{k,\sigma}(z) \right|^2 \right) dz. \tag{12}$$

In this model, we assume that the minimum spacing between channels can be considered as sufficient to neglect the effect of the beat frequency between channels [20]. In fact, ITU standard fiber optic telecommunication for 16, 32, or 48 channels is typically 100 and 50 GHz. This approximation leads to

$$\begin{aligned} &\sum_\sigma S^{\pm}_{k,\sigma} \\ &\quad \approx \frac{1}{v_g \Delta z_k} \int_{z_k^-}^{z_k^+} \cdot \left(\sum_\sigma \frac{1}{E_\sigma} \left| F^+_{k,\sigma}(z) \right|^2 + \sum_\sigma \frac{1}{E_\sigma} \left| F^-_{k,\sigma}(z) \right|^2 \right) dz \\ &\quad = \sum_i S^+_{k,i} + \sum_j S^-_{k,j}. \end{aligned} \tag{13}$$

The average ASE photon density in the kth section $S_{\text{spon},k,m}$ is calculated [15]–[17], [20] as

$$\begin{aligned} &S_{\text{spon},k,m} \\ &\quad = \frac{1}{v_g E_m \Delta z_k} \int_{z_k^-}^{z_k^+} \left(I^+_{\text{spon},k,m}(z) + I^-_{\text{spon},k,m}(z) \right) dz \\ &\quad = \frac{R_{\text{spon},k}}{v_g g_{n,k,m}} \cdot \left(\frac{(\exp(g_{n,k,m}\Delta z_k) - 1)(C^+_{k,m} + C^-_{k,m})}{g_{n,k,m}\Delta z_k} - 2 \right). \end{aligned} \tag{14}$$

The integration constants can be calculated by using the boundary conditions

$$\left.\begin{aligned} I^+_{\text{spon},k,m}(z^-_k) &= I^+_{\text{spon},k-1,m}(z^+_{k-1}) \quad \text{for } \boldsymbol{k \neq 1} \\ I^-_{\text{spon},k,m}(z^+_k) &= I^-_{\text{spon},k+1,m}(z^-_{k+1}) \quad \text{for } \boldsymbol{k \neq M} \\ I^-_{\text{spon},M,m}(z^+_M = L) &= R_2 I^+_{\text{spon},M,m}(z^+_M) \quad \text{for } \boldsymbol{k = M} \\ I^+_{\text{spon},1,m}(z^-_1 = 0) &= R_1 I^-_{\text{spon},1,m}(z^-_1) \quad \text{for } \boldsymbol{k = 1} \end{aligned}\right\}. \tag{15}$$

Equation (15) can be written under a matrix form, $M.\boldsymbol{C} = \delta$ as shown in (16) at the bottom of the page where

$$\delta_k = -\frac{\beta_m R_{\text{spon},k} E_m}{2 g_{n,k,m}}, \quad \alpha_k = -\delta_k \exp(g_{n,k,m}\Delta z_k).$$

The determinant of matrix $\boldsymbol{M}$

$$\begin{aligned} &\det(\boldsymbol{M}) \\ &\quad = \left(\prod_{j=1}^{M} \delta_j^2 \right) \left(1 - R_1 R_2 \left(\prod_{j=1}^{M} \exp(2 g_{n,j,m} \Delta z_j) \right) \right) \end{aligned} \tag{17}$$

where

$$\left(1 - R_1 R_2 \left(\prod_{j=1}^{M} \exp(2 g_{n,j,m} \Delta z_j) \right) \right)$$

is the laser gain threshold condition which is different from zero for a low facets reflectivities SOA. The analytical expression of $C^{\pm}_{k,m}$ can then be obtained by the inversion of matrix $\boldsymbol{M}$.

B. Electron Rate Equations and Equivalent Circuit

A rate equation model is used to describe the dynamics of the carrier concentrations in each section

$$\begin{aligned} \frac{dN_k}{dt} &= \frac{I_k}{q_e \Delta z_k w d} - R(N_k) - v_g \\ &\quad \cdot \left(\sum_{i,\,\text{modes}} \beta_i g_{m,k,i} S_{\text{spon},k,i} - \sum_i g_{m,k,i} S^{\pm}_{k,i} \right) \end{aligned} \tag{18}$$

where I_k is the current into the active region of the section. q_e is the electron charge. $R(N_k)$ is the total spontaneous recombina-

$$\left(\begin{array}{ccccccc|ccccccc} \alpha_1 & \delta_2 & 0 & \cdot & \cdot & \cdot & \cdot & \cdot & \cdot & \cdot & \cdot & \cdot & \cdot & 0 \\ 0 & \alpha_2 & \delta_3 & 0 & \cdot & \cdot & \cdot & \cdot & \cdot & \cdot & \cdot & \cdot & \cdot & \cdot \\ 0 & 0 & \alpha_3 & \delta_4 & 0 & \cdot & & \cdot & \cdot & \cdot & \cdot & \cdot & \cdot & \cdot \\ \cdot & \cdot & \cdot & \cdot & \cdot & \cdot & \cdot & \cdot & \cdot & \cdot & \cdot & \cdot & \cdot & \cdot \\ 0 & \cdot & \cdot & 0 & \alpha_k & \delta_{k+1} & 0 & \cdot & \cdot & \cdot & \cdot & \cdot & \cdot & 0 \\ \cdot & \cdot & \cdot & \cdot & \cdot & \cdot & \cdot & \cdot & \cdot & \cdot & \cdot & \cdot & \cdot & \cdot \\ 0 & \cdot & \cdot & \cdot & 0 & 0 & R_2\alpha_M & \delta_M & 0 & \cdot & \cdot & \cdot & \cdot & 0 \\ \hline 0 & \cdot & \cdot & \cdot & \cdot & 0 & 0 & \alpha_M & \delta_{M-1} & 0 & \cdot & \cdot & \cdot & 0 \\ \cdot & \cdot & \cdot & \cdot & \cdot & \cdot & \cdot & \cdot & \cdot & \cdot & \cdot & \cdot & \cdot & \cdot \\ 0 & \cdot & \cdot & \cdot & \cdot & \cdot & \cdot & 0 & 0 & \alpha_k & \delta_{k-1} & \cdot & \cdot & 0 \\ \cdot & \cdot & \cdot & \cdot & \cdot & \cdot & \cdot & \cdot & \cdot & \cdot & \cdot & \cdot & \cdot & \cdot \\ 0 & \cdot & \cdot & \cdot & \cdot & \cdot & \cdot & \cdot & \cdot & \cdot & 0 & \alpha_3 & \delta_2 & 0 \\ 0 & \cdot & \cdot & \cdot & \cdot & \cdot & \cdot & \cdot & \cdot & \cdot & \cdot & 0 & \alpha_2 & \delta_1 \\ \delta_1 & 0 & \cdot & \cdot & \cdot & \cdot & \cdot & \cdot & \cdot & \cdot & \cdot & 0 & 0 & R_1\alpha_1 \end{array}\right) \left(\begin{array}{c} C^+_{1,m} \\ C^+_{2,m} \\ C^+_{3,m} \\ \cdot \\ C^+_{k,m} \\ \cdot \\ C^+_{M,m} \\ C^-_{M,m} \\ \cdot \\ C^-_{k,m} \\ \cdot \\ C^-_{3,m} \\ C^-_{2,m} \\ C^-_{1,m} \end{array}\right) = \left(\begin{array}{c} \delta_2 - \delta_1 \\ \delta_3 - \delta_2 \\ \delta_4 - \delta_3 \\ \cdot \\ \delta_{k+1} - \delta_k \\ \cdot \\ \delta_M - R_2\delta_M \\ \delta_{M-1} - \delta_M \\ \cdot \\ \delta_{k-1} - \delta_k \\ \cdot \\ \delta_2 - \delta_3 \\ \delta_1 - \delta_2 \\ \delta_1 - R_1\delta_1 \end{array}\right). \tag{16}$$

tion rate of the electrons given by $R(N_k) = A_{nr}N_k + B_sN_k^2 + C_{au}N_k^3$ where A_{nr}, B_s, and C_{au} are spontaneous electron recombination coefficients. In (18) the analytical expressions of $R(N_k)$, $S_{\text{spon},k}$, and $S_{k,i}^{\pm}$ are established. In that way, for a set of injection currents and input signals propagating along the z-axis, respectively in the positive and the negative direction, the performances of the amplifier are completely determined by M carrier densities, obtained by solving together M equations.

This approach permits to use electrical circuit simulator for the calculation of N_k. This leads to the transformation of the M rate equations under the form of an equivalent circuit model. The carrier density N is related to the voltage V of the SOA through Boltzmann's statistics

$$N = N_e e^{V/U_T} \tag{19}$$

where

N_e	equilibrium electron density;
$U_T = \eta KT/q_e$	where K is Boltzmann's constant;
T	absolute temperature;
η	factor of ideality.

The equivalent circuit in the kth section is then obtained from (18) and (19) and can be described by

$$C_k\frac{dV_k}{dt} = I_k - I_{\text{rec},k} - \sum_{i,\,\text{modes}} I_{\text{spon},k,i} - \sum_i I_{i,k}^{\pm} \tag{20}$$

where

$$C_k = (q_e\Delta z_k wd)N_k/U_T$$
$$I_{\text{rec},k} = (q_e\Delta z_k wd)R(N_k)$$
$$I_{\text{spon},k,i} = (q_e\Delta z_k wd)\beta_i v_g g_{m,k,i}S_{\text{spon},k,i}$$

and

$$I_i^{\pm} = (q_e\Delta z_k wd)v_g g_{m,k,i}S_{k,i}^{\pm}.$$

The simulation is achieved on a microwave simulator (MDS of Hewlett-Packard) where dc, ac, time domains, and nonlinear (harmonic balance method) simulations can be performed [21]–[23].

III. Analysis of Inline Photodetection in Presence of Bidirectional Transmission

A. Principle of Simultaneous Photodetection

For a multi-electrode SOA, using the first sections beside an incident optical signal as a preamplifier and the last section as a detector–amplifier can perform the detection operation. In the presence of contrapropagating incident signals of same level, we will detect both signals at the contact of the last section, but the signal which benefits more from the preamplifier cavity sections gain, will have a higher photodetection level [12] (Fig. 2). The signal detection can be performed over all the SOA spectral -3 dB bandwidth, which is interesting in WDM applications. The experimental verification of this application is obtained by using a three-electrode SOA.

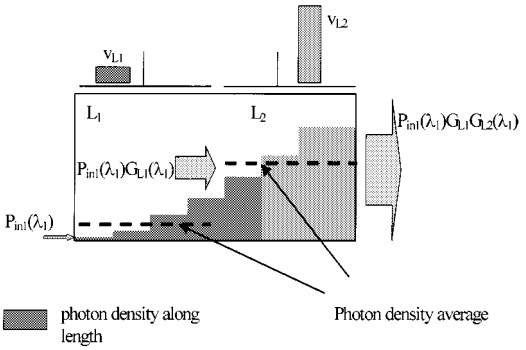

Fig. 2. Diagram showing change in photon density along length and photodetection response at contact L_1 and L_2 in a two-section SOA.

B. Photodetection Responses

The analytical expression of the photodetected response at the kth-section $v_{\omega,k}$ can be obtained by using small-signal analysis of the rate (18) [22], [23], [25]

$$v_{\omega,k} = \sum_i v_{\omega,k,i} = \frac{1}{T_kY_k}\left(-\sum_i Z_{i1,k}p_{im} - \sum_{j,\,j\neq k}^{M} Z_{i2,j}v_{\omega,j}\right) \tag{21}$$

where p_{im} is the small signal SOA optical input power

$$V_{ol,k} = \Delta z_k wd,\ T_k = (1 + j\omega\tau_k),\ Y_k = \frac{C_{1k}}{\tau_k}$$

where

$$\tau_k = \left(\frac{\partial}{\partial N_k}\left(R_k + v_g\left(\sum_{i,\,\text{modes}}\beta_i g_{m,k,i}S_{\text{spon},k,i} + \sum_i g_{m,k,i}S_{k,i}^{\pm}\right)\right)\Bigg|_{N_k=N_{0,k}}\right)^{-1}$$

$$C_{1k} = q_eV_{ol,k}\left.\frac{\partial N_k}{\partial V_k}\right|_{V_k=V_{0,k}}$$

$$Z_{i_{1,k}} = q_eV_{ol,k}v_g\sum_i g_{m,k,i}\frac{S_{k,i}^{\pm}}{P_{\text{in}0,i}}$$

$$Z_{i_{2,j}} = C_{1j}v_g\frac{\partial}{\partial N_j}\left(\sum_{i,\,\text{modes}}\beta_i g_{m,k,i}S_{\text{spon},k,i} + \sum_i g_{m,k,i}S_{k,i}^{\pm}\right)\Bigg|_{N_j=N_{0,j}}$$

where

$$C_{1j} = q_eV_{ol,k}\left.\frac{\partial N_j}{\partial V_j}\right|_{V_j=V_{0,j}}$$

and quantities with a zero subscript indicate steady state values.

The first term of the photodetected response in (21), $-(1/T_kY_k)(\sum_i Z_{i1,k}p_{im})$, is related to the variation of the input optical signals. The last term $-(1/T_kY_k)(\sum_{j,\,j\neq k}^{M} Z_{i2,j}v_{\omega,j})$ takes into account the cross gain modulation in the other sections between signals on the one hand and between ESA and signals, on the other hand.

For an electrode constituted of θ sections of equal length, the photodetected voltage at this electrode is given by

$$v_\omega = \frac{1}{\theta} \sum_{k=\gamma}^{\theta+\gamma-1} v_{\omega,k}. \tag{22}$$

C. Definition of the Crosstalk

By using a multi-electrode SOA, the photodetected voltage in presence of two simultaneous contrapropagating input optical signals where $P_{\mathbf{in},1}(\lambda_1)$ (coming in the positive z-direction) and $P_{\mathbf{in},2}(\lambda_2)$ (coming in negative z-direction) is the sum of $v_\omega(\lambda_1)$ and $v_\omega(\lambda_2)$. We consider that the frequency of the two bidirectional optical input signals is lower than SOA photodetection bandwidth ($\omega\tau_k < 1$). By assuming that $v_\omega(\lambda_2)$ is the interfering signal, we defined the crosstalk by the ratio of $v_\omega(\lambda_2)/v_\omega(\lambda_1)$. By taking $R_1 = R_2 = 0$, $g_{n,k,i} = g_{m,k,i}$ and $\lambda_1 = \lambda_2$, the crosstalk expression can be written from (9), (11), (21), and (22) as

$$C_R = \frac{v_\omega(\lambda_2)}{v_\omega(\lambda_1)} \approx \frac{\sum_{k=\gamma}^{\theta+\gamma-1} \left(Z_{21,k} p_{2m} + \sum_{j,\, j\neq k}^{M} Z_{i2,j} v_{\omega,j} \right)}{\sum_{k=\gamma}^{\theta+\gamma-1} \left(Z_{11,k} p_{1m} + \sum_{j,\, j\neq k}^{M} Z_{i2,j} v_{\omega,j} \right)}$$

$$C_R = \frac{\sum_{k=\gamma}^{\theta+\gamma-1} \left(\Gamma q_e p_{2m} \left(1 - G_{si,k}^{-1}\right) \prod_{j=k}^{M} G_{si,j} + \sum_{j,\, j\neq k}^{M} Z_{i2,j} v_{\omega,j} \right)}{\sum_{k=\gamma}^{\theta+\gamma-1} \left(\Gamma q_e p_{1m} \left(1 - G_{si,k}^{-1}\right) \prod_{j=1}^{k} G_{si,j} + \sum_{j,\, j\neq k}^{M} Z_{i2,j} v_{\omega,j} \right)}. \tag{23}$$

By detecting at the extremity electrode and by assuming for simplicity that the electrode is modeled by one section ($k = M$), in this case, (23) leads to

$$C_R = \frac{p_{2m}(1 + \Omega/p_{2m})}{p_{1m} \prod_{j=1}^{M-1} G_{si,j} \left(1 + \Omega \Big/ \left(p_{1m} \prod_{j=1}^{M-1} G_{si,j} \right)\right)} \tag{24}$$

where

$$\Omega = \frac{\sum_{j,\, j\neq k}^{M} Z_{i2,j} v_{\omega,j}}{\Gamma q_e (G_{si,k} - 1)}.$$

For lower optical power, the cross gain modulation term becomes negligible ($\Omega \to 0$) and in this case, (24) tends to

$$C_R = \frac{p_{2m}}{p_{1m} \prod_{j=1}^{M-1} G_{si,j}}$$

which is the amplitude ratio of the bidirectional optical incident signals at the considered electrode.

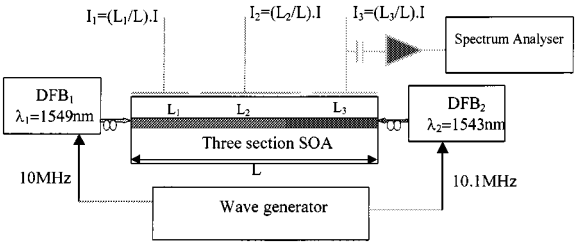

Fig. 3. Experimental setup of photodetection in presence of bidirectional transmission. (I: total SOA bias current.)

IV. Bidirectional Photodetection Experimental Setup

The used SOA is a three-electrode with 100-200-100 μm electrodes length. It is a ridge waveguide structure, AR-coated with 7° angled facet. For a bias current of 150 mA, the fiber to fiber gain for the TE mode is typically 12 dB. The peak gain wavelength is 1520 nm with an optical bandwidth of 70 nm and the 3 dB saturation output power is about 7 dBm. A schematic of the setup is shown in Fig. 3. The contrapropagating signals are obtained by directly modulating two DFB lasers, DFB_1 at $\lambda_1 = 1549$ nm and DFB_2 at $\lambda_2 = 1543$ nm, by a wave generator. The modulation index of both input optical signals is typically $m = 0.1$. The two signals are directed to the SOA via a polarization controller and a fiber coupler. The photodetected signals are obtained at the extremity 100 μm electrode length and sent to an electrical spectrum analyzer after an electrical amplification of about 28 dB gain.

V. Results

The parameters for the amplifier used in the numerical simulation are given in Table I. For crosstalk measurements, DFB_1 is modulated at $f_1 = 10$ MHz and DFB_2 at $f_2 = 10.1$ MHz to separate the contribution of the two contrapropagating input signal responses at the spectrum analysis. Harmonic balance method is used for the computational results, which permits to obtain the photodetected response at f_1 and f_2. The experimental and the simulations results are performed by taking identical optical input powers ($P_{\mathbf{in},1} = P_{\mathbf{in},2}$, and $p_{1m} = p_{2m} = p_m$). The three SOA contacts are biased by the same current density. Figs. 4 and 5 show the crosstalk level as a function of SOA bias current. For input optical signals at -5 and -10 dBm, measurements and simulation present a dip in crosstalk. In fact, the numerator term $(1 + \Omega/p_m)$ in (24) can be equal to zero ($v_{\omega,j} < 0$). Actually, we can see in (24) that the numerator term cancel earlier than the denominator term because Ω is divided by

$$\left(p_m \prod_{j=1}^{M-1} G_{si,j} \right)$$

instead of p_m. In fact, the crosstalk dip level is due to the cross gain modulation in the other section between the contrapropagating signals. This cross gain modulation can cancel the photodetected response of the contradirectional signal, which has not benefited from of the preamplifier sections. In this case, a free crosstalk response can be obtained for certain operating conditions. By reducing the optical input powers, the crosstalk at the dip level shifts to high bias current. After the dip level,

TABLE I
LIST OF PARAMETER VALUES

Symbol	Parameter	Value
$g_{m,k}=a(N_k-N_0)-\kappa[\lambda_i-(\lambda_0+\delta\lambda(N_k-N_{th}))]^2$		
a	Gain factor	$1.75\ 10^{-20}$ m²
N_0	Carrier density at transparence	$1.55\ 10^{24}$ m^{-3}
κ	Curvature of the spectral gain	$4\ 10^{18}$ m^{-3}
λ_0	Gain peak frequency	1560 nm
$\delta\lambda$	Frequency shift coefficient	$2.5\ 10^{-}32$ m^4
N_{th}	Reference carrier density	$2.8\ 10^{24}$ m^{-3}
A_{nr}	Recombination factor	10^{8} s^{-1}
B_s	Recombination factor	10^{-16} m^{3}s^{-1}
C_{au}	Recombination factor	$8\ 10^{-41}$ m^{6}s^{-1}
d	Active layer thickness	0.12 μm
W	Active region width	2 μm
L	Amplifier length	400μm
	Amplifier electrodes length	(100+200+100)
Δz_k	Section length	100μm
α	Internal loss	3000 m^{-1}
Γ	Confinement factor	0.35
$R_{1,2}$	Residual facet reflectivity	$5\ 10^{-5}$
β_i	Spontaneous emission factor	$5\ 10^{-5}$

the crosstalk increased in function of the bias current. For lower optical power (Fig. 6), the cross gain modulation term becomes negligible and (24) tends to

$$C_R = \left(\prod_{j=1}^{M-1} G_{si,j} \right)^{-1}$$

which indicates that the crosstalk in presence of simultaneous bidirectional wavelength can be reduced by increasing the SOA preamplifier sections.

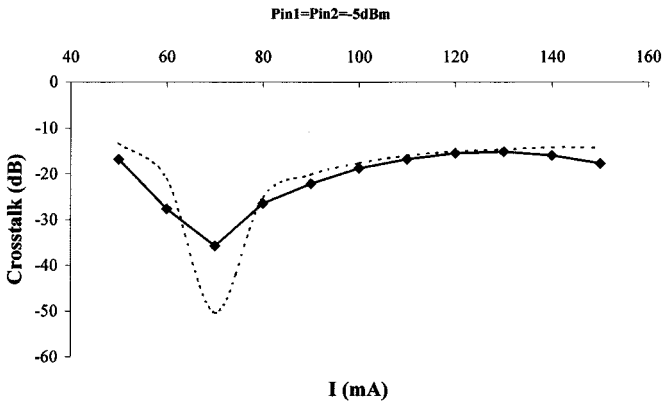

Fig. 4. Crosstalk versus SOA bias current for two optical contrapropagating signals of average power of about -5 dBm. Crosstalk (dB) $= 20\log(v_\omega(\lambda_2)/v_\omega(\lambda_1))$.

VI. CONCLUSION

A rate equation model for static and dynamic behavior for bidirectional transmission in a multisection SOA has been developed. The rate equations for each section have been implemented on an electrical simulator, (MDS of Hewlett Packard). Electrical simulators permit easy use of dc, ac, or time domains simulations and they grant easy handling of parasitic contributions and integration with electrical circuit components. This approach of SOA modeling, M differential equations for M sections, permits also the use of behavioral modeling tools, like VHDL-AMS, for simultaneous simulation of completely different devices [26]. The Small signal photodetection response in presence of co and contrapropagating signals in a multisection SOA's has been given. The photodetection crosstalk ex-

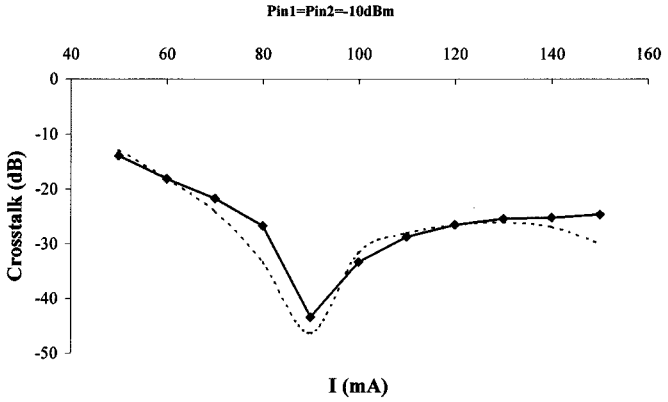

Fig. 5. Crosstalk versus SOA bias current for two optical contra propagating signals of average power of about -10 dBm. Crosstalk (dB) $= 20\log(v_\omega(\lambda_2)/v_\omega(\lambda_1))$.

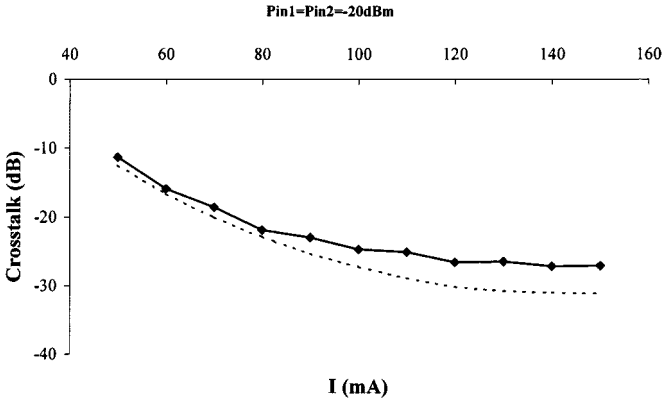

Fig. 6. Crosstalk versus SOA bias current for two optical contra propagating signals of average power of about -20 dBm. Crosstalk (dB) $= 20\log(v_\omega(\lambda_2)/v_\omega(\lambda_1))$.

pression in optical duplex transmission has also been reported. Simultaneous bidirectional photodetection experiments using a three-electrode SOA show good agreement between measured crosstalk and simulated results obtained by harmonic balance method. A photodetection response nearly free of crosstalk has been obtained for certain operating conditions, due to the cross gain modulation between contrapropagating signals. The influence of crosstalk on systems performances has been studied [27], [28]. A crosstalk of -7 dB presents a penalty of about 1dB for a PIN receiver. This result can be used for an SOA by assuming that the SOA noise is not dependent on incident light power. The general case could be carried out in a future work to evaluate the required crosstalk for simultaneous photodetection by the use of a multi-electrode SOA in optical duplex transmission.

ACKNOWLEDGMENT

The authors wish to thank Prof. J. Le Bihan, Head of the RESO Laboratory at Ecole Nationale d'Ingénieurs de Brest (ENIB), for his support and encouragement.

REFERENCES

[1] A. Sharaiha, H.-W. Li, J. Le Bihan, and F. Ropars, "Analysis of the operation of a bi-directional bus made of two semiconductor laser amplifiers running up to 1.555Gb/s," *Microwave Optic. Technol. Lett., MOTL*, vol. 13, no. 4, pp. 240–242, Nov. 1996.

[2] K. Bertilsson, R. Rörgen, P. A. Andrekson, and S. T. Eng, "Characterization of an InGaAsP semiconductor laser amplifier as a multifunctional device," *J. Lightwave Technol.*, vol. 11, pp. 1147–1150, July 1993.

[3] R. Fortenberry, A. J. Lowery, W. L. Ha, and R. S. Tucker, "Photonic packet switch using semiconductor optical amplifier," *Electron. Lett.*, vol. 27, no. 14, pp. 1305–1307, 1991.

[4] M. Eislet, G. Groβkopff, R. Ludwig, W. Pieper, and H. G. Weber, "Photonic ATM switching with semiconductor laser amplifier gates," *Electron. Lett.*, vol. 28, no. 15, pp. 1438–1439, 1992.

[5] R. F. Kalman, L. G. Kazovsky, and J. W. Goodman, "Space division switches based on semiconductor optical amplifiers," *IEEE Photon. Technol. Lett.*, vol. 4, pp. 1048–1051, Sept. 1992.

[6] M. Renaud, "Semiconductor optical amplifier gate arrays: Devices and applications," in *Proc. IEEE Lasers Electro-Optics Soc. (LEOS'98)*, Orlando, FL, Dec. 1998, Paper THV1, pp. 190–191.

[7] T. Durhuus, B. MikKelsen, C. Joergensen, S. L. Danielsen, and K. E. Stubkjaer, "All-optical wavelength conversion by semiconductor optical amplifier," *J. Lightwave Technol.*, vol. 14, pp. 942–954, June 1996.

[8] K. Obermann, S. Kindt, D. Bruer, and K. Petermann, "Performance analysis of wavelength converters based on cross-gain modulation in semiconductor optical amplifier," *J. Lightwave Technol.*, vol. 16, pp. 78–85, Jan. 1998.

[9] A. Sharaiha, H.W. Li, F. Marchèse, and J. Le Bihan, "All-optical logic NOR gate using a semiconductor laser amplifier," *Electron. Lett.*, vol. 33, no. 4, pp. 323–324, 1997.

[10] T. Rampone, H. W. Li, and A. Sharaiha, "Semiconductor optical amplifier used as in-line optical detector with conservation of the signal DC-component," *J. Lightwave Technol.*, vol. 16, July 1998.

[11] G. Giuliani, P. Cinguino, and V. Seano, "Multifunctional characteristics of 1.5 μm two-section amplifier-modulator-detector SOA," *IEEE Photon. Technol. Lett.*, vol. 8, pp. 367–369, Mar. 1996.

[12] R. M. Fortenberry, A. J. Lowery, and R. S. Tucker, "Up to 16 dB improvement in detected voltage using two section semiconductor optical amplifier detector," *Electron. Lett.*, vol. 28, no. 5, pp. 474–475, Feb. 1992.

[13] L. Gillner, "Small-signal modulation of a two-section semiconductor laser amplifier: Pure PM response," *IEEE Photon. Technol. Lett.*, vol. 3, no. 5, pp. 445–447, 1991.

[14] A. Sharaiha, "Simultaneous in-line photodetection using semiconductor optical amplifier in presence of bi-directional transmission," in *IEEE Lasers Electro-Optics Society (LEOS'98)*, Orlando, FL, December 1998, Paper WT3, pp. 303–304.

[15] M. J. Adams, J. V. Collins, and I. D. Henning, "Analysis of semiconductor laser optical amplifiers," *Inst. Elec. Eng Proc.—J*, vol. 132, no. 1, pp. 58–63, 1985.

[16] L. Gillner, "Modulation properties of a near travelling wave semiconductor laser amplifier," *Inst. Elec. Eng. Proc.—J*, vol. 139, no. 5, pp. 331–338, 1992.

[17] M. J. Adams, "Theory of two section laser amplifiers," *Optic. Quantum Electron.*, vol. 21, pp. S15–S31, 1989.

[18] P. Brosson, "Analytical model of semiconductor optical amplifier," *J. Lightwave Technol.*, vol. 12, pp. 49–54, Jan. 1994.

[19] C. Y. J. Chu and H. Ghafouri-shiraz, "Analysis of gain and saturation characteristics of a semiconductor laser amplifier using transfer matrix," *J. Lightwave Technol.*, vol. 12, pp. 1378–1386, Aug. 1994.

[20] T. Durhuus, B. Mikkelsen, and K. E. Stubkjaer, "Detailled dynamic model for semiconductor optical amplifier and their crosstalk and intermodulation distortion," *J. Lightwave Technol.*, vol. 10, pp. 1056–1064, Aug. 1992.

[21] L. D. Westbrook, "Simulation of semiconductor laser amplifiers using harmonic balance," *Electron. Lett.*, vol. 28, no. 525, pp. 2348–2349, 1992.

[22] A. Sharaiha, "Harmonic and intermodulation distortion analysis by perturbation and harmonic balance methods for in-line photodetection in a semiconductor optical amplifier," *IEEE Photon. Technol. Lett.*, vol. 10, pp. 421–423, Mar. 1998.

[23] ——, "Distortion analysis of the photodetection and gain spectral responses of a semiconductor optical amplifier," *IEEE Photon. Technol. Lett.*, vol. 10, pp. 1301–1303, Sept. 1998.

[24] Y. Boucher, "Transfer matrix of ad Dirac-like singularity of the dielectric permitttivity," *IEEE J. Quantum Electron.*, vol. 33, no. 2, pp. 265–268, 1997.
[25] M. Gustavsson, A. Karlson, and L. Thylèn, "Traveling wave semiconductor laser amplifier detectors," *J. Lightwave Technol.*, vol. 8, no. 4, pp. 610–617, 1990.
[26] J. Morikuni, G. Dare, P. Mena, A. Harton, and K. Wyatt, "Simulation of optical interconnect devices, circuits, and systems using analog behavioral modeling tools," in *Proc. IEEE Lasers Electro-Optics Society (LEOS'98)*, Orlando, FL, Dec. 1998, Paper Wk5, pp. 235–236.
[27] P. Granestrand, L. Thylèn, and G. Wicklund, "Analysis of switching employing a 4×4 switch matrix: Crosstalk requirements and system proposal," in *Proc. ECOC'89*, 1989, Paper WeA15-4.
[28] P. P. Bohn and S. K. Das, "Return loss requirements for optical duplex transmission," *J. Lightwave Technol.*, vol. LT-5, pp. 243–254, Feb. 1987.

A. Sharaiha was born on March 6, 1956 in Amman, Jordan. He received the B.S. degree (Maîtrise EEA) in 1980, the Diplôme d'Etudes Approfondies (DEA) in 1981, and Ph.D degree in 1984, all from University of Rennes I, France.

From 1981 to 1989, he was engaged in signal processing and instrumentation systems for dielectric measurements. In 1989, he joined the RESO Laboratory at Ecole Nationale d'Ingénieurs de Brest, France, as a Maître de Conférences. His main fields of interest include semiconductor optical amplifier as a multifunctional device, optical communication systems, and integrated circuits for high bit data rate applications.

M. Guegan was born in Lannion, France, in 1973. He received the B.S. degree in Physics ("Maîtrise de Physique") in 1996 and the D.E.A. ("Diplôme d'Etudes Approfondies") in 1997, all from the University of Bretagne Occidentale, Brest, France.

In 1999, he joined the RESO Laboratory at the Ecole Nationale d'Ingénieurs de Brest, France, as a Ph.D. student. His main fields of interest include semiconductor optical amplifiers (SOA's) as a multifunctional device, specially multi-electrodes SOA's, and optical communication systems.